

Optical micro-shadowgraph-based method for measuring micro-solderball height

Shihua Wang
Chenggen Quan
Cho Jui Tay

National University of Singapore
Department of Mechanical Engineering
10 Kent Ridge Crescent
Singapore, 119260

Abstract. An optical micro-shadowgraph for the height measurement of a micro-solderball on a semiconductor wafer is proposed. The micro-shadow image resulting from an oblique illumination onto the protruded solderball/bump on the wafer is clearly captured. Experimental investigation shows that accurate solderball height measurement can be readily obtained. © 2005 Society of Photo-Optical Instrumentation Engineers. [DOI: 10.1117/1.1906003]

Subject terms: geometrical optics; metrology; microscopy; optical shadowgraphs; semiconductor wafers; micro-solderballs.

Paper L040542R received Aug. 11, 2004; revised manuscript received Dec. 29, 2004; accepted for publication Feb. 22, 2005; appeared online Feb. 23, 2005; published online May 23, 2005.

The reliability of the solder joint/solderball in the micro-ball grid array (micro-BGA)¹ has been observed to be highly dependent on the height uniformity/coplanarity² of the micro-solderballs across the wafer. To obtain the height information from a micro-BGA on a silicon wafer, we explore a simple but effective method using the inherent shadow phenomenon of an object illuminated by an oblique illumination.

Figure 1 shows a schematic of a micro-solderball/bump illuminated by an incident beam of angle θ . The image plane of the CCD sensor in the X-Y plane is parallel to the line AD and perpendicular to the reflected light. A lens would direct the resulting shadow onto the CCD sensor and hence a typical shadow and projection image of a micro-solderball in the X-Y plane can be illustrated as an overlapped shadow pattern. The length of both d and L can be measured, where d is the diameter of the bump and L is the total length across the bump and its shadow. Hence, from Rt $\triangle ACD$, we have

$$\sin 2\theta = \frac{\overline{AD}}{\overline{AC}} = \frac{\overline{A'D'}/\beta}{\overline{AC}} = \frac{L/\beta}{\overline{AC}}, \quad (1)$$

$$\overline{AC} = \frac{L}{\beta \cdot \sin 2\theta}, \quad (2)$$

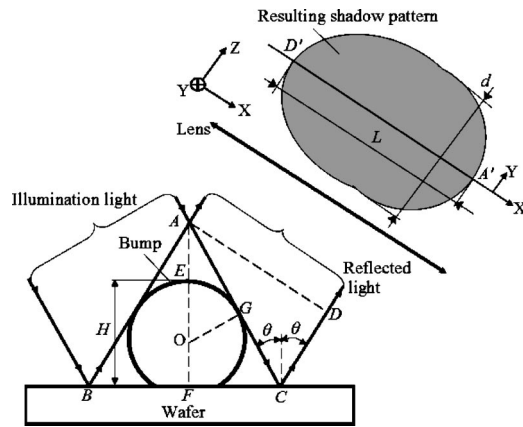


Fig. 1 Cross-section view of the bump and corresponding shadow pattern on the CCD sensor located in the X-Y plane.

where β is magnification of the microscopic system. From Rt $\triangle AOG$,

$$(\overline{AE} + \overline{EO}) \sin \theta = \overline{GO}, \quad (3)$$

where $\overline{EO} = \overline{GO} = d/2\beta$. We have

$$\overline{AE} = \frac{d}{2\beta \cdot \sin \theta} - \frac{d}{2\beta}, \quad (4)$$

and from Rt $\triangle AFC$, we have

$$\overline{AF} = \overline{AC} \cos \theta. \quad (5)$$

Substituting Eqs. (2), (4), and (5) into $H = \overline{AF} - \overline{AE}$, the height of the solderball is given by:

$$H = \frac{1}{2\beta \sin \theta} [L - (1 - \sin \theta) \cdot d]. \quad (6)$$

In Fig. 2, light from a halogen lamp passes through a collimating lens 1 and is directed onto a focusing lens 2. The light beam emerging from lens 2 is focused onto an aperture stop 1. A telecentric illumination consisting of lens 1, lens 2, stop 1, and lens 3 enables illumination with collimated light over the test surface.³ Note that lens 3 (semi-lens) allows the illumination angle to be easily adjusted by selecting illumination axis offset (P) and most of the light

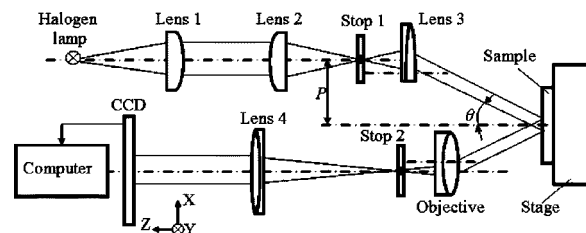


Fig. 2 System configuration.

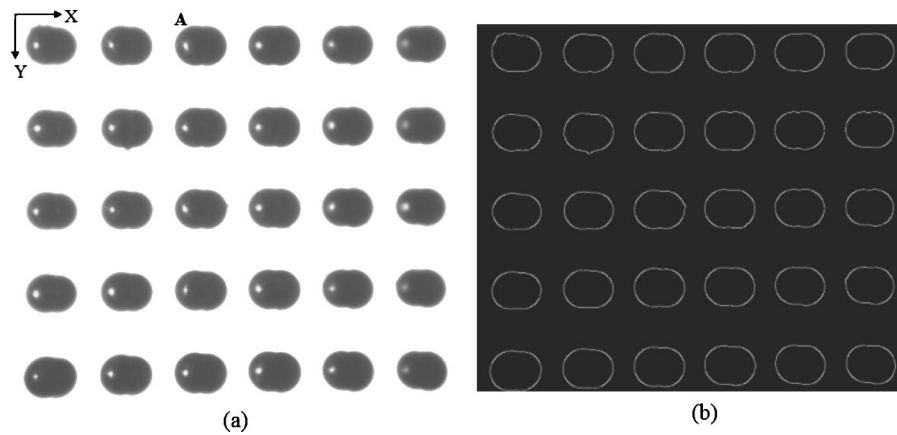


Fig. 3 Results of (a) a shadow image of bumps on a wafer, (b) edge contour of those bumps obtained through image processing using Canny's method.

is reflected in the specular direction as the test surface (silicon wafer) is mirror-like.⁴ To capture the resulting shadow pattern, another telecentric microscope consisting of an objective (focal length $f_o=20$ mm), aperture stop 2, and lens 4 (focal length $f_4=100$ mm) is aligned in the specular direction of the reflected light. This arrangement ensures an optimal contrast of the recorded white-black pattern on a CCD sensor Stop 2 located at the focal plane of the lens 4 ensures that rays primarily parallel to the optical axis reach the CCD sensor. The resulting shadow pattern is recorded through a frame grabber for the further processing.

Figure 3(a) shows a typical shadow pattern of micro-solderballs on a wafer. It is seen that those shadows are elongated in the X direction. To determine the shadow contour, Canny's edge method⁵ was applied to the above shadow pattern. Figure 3(b) shows the edges/contours of those shadows. As shown in Fig. 3(b), the shadow edges have been located and the corresponding shadow length is correlated to the micro-solderball/bump height. For example, the edge locations across the centroids of a specific bump A and its shadow length along the Y direction have been used to measure the bump diameter d ($=58$ pixels) and the elongated shadow along the X direction in a length of L ($=75$ pixels) was also obtained. Based on Eq. (6), the bump height of $108 \mu\text{m}$ was determined. Similarly, individual height of each bump on the wafer can be measured accordingly. For those bumps in Fig. 3, the bump height variation (uniformity/coplanarity) was evaluated using a statistical parameter of standard deviation σ to be $\pm 4.8 \mu\text{m}$. To verify the accuracy of the proposed method, the height ($108.2 \mu\text{m}$) of bump A was obtained using a commercial WYKO profiler (Model: Wyko NT 3300, a white-light interferometric profiler). Compared to the height ($108 \mu\text{m}$) obtained by the proposed method, the discrepancy is less than 0.2%. According to the ISO guide,⁶ the combined standard uncertainty $u_c(H)$ attributed to H based on Eq. (6) is given as follows:

$$u_c(H) = \left[\left(\frac{\partial H}{\partial L} \right)^2 u_{(L)}^2 + \left(\frac{\partial H}{\partial d} \right)^2 u_{(d)}^2 + \left(\frac{\partial H}{\partial \beta} \right)^2 u_{(\beta)}^2 + \left(\frac{\partial H}{\partial \theta} \right)^2 u_{(\theta)}^2 \right]^{1/2}, \quad (7)$$

where the partial derivatives ($\partial H/\partial L=0.3$, $\partial H/\partial d=0.2$, $\partial H/\partial \beta=22$, and $\partial H/\partial \theta=137$) for bump A are called sensitivity coefficients, $u_{(L)}$, $u_{(d)}$, $u_{(\beta)}$ and $u_{(\theta)}$ are the standard uncertainties of L , d , β , and θ , respectively. The error resulting from determination of those lengths of L and d are less than 1 pixel ($10 \mu\text{m}$) which is $2 \mu\text{m}$ on the test surface while the magnification (β) is $5\times$. The corresponding standard uncertainties assuming a rectangular distribution are given approximately by $u_{(L)}=u_{(d)}=2/\sqrt{3}=1.2 \mu\text{m}$. The magnification ($\beta=5\times$) is in a tolerance of $\pm 0.05\times$ with standard uncertainty $u_{(\beta)}=0.05/\sqrt{3}=0.03\times$. The error resulting from illumination angle uncertainty was estimated to be in the range of ± 1 deg (0.02 rad) and the corresponding standard uncertainty is given by $u_{(\theta)}=0.02/\sqrt{3}=0.01$ rad. The combined standard uncertainty $u_c(H)$ in Eq. (7) can be calculated as follows:

$$u_c(H) = (0.3^2 \times 1.2^2 + 0.2^2 \times 1.2^2 + 22^2 \times 0.05^2 + 137^2 \times 0.01^2)^{1/2} = 1.8 \mu\text{m}. \quad (8)$$

In summary, the proposed microscopic system is feasible to do measurement on the height of the smooth and curved micro-solderball. The results presented in this letter demonstrate the potential of the proposed method to be a practical tool for in-situ inspection of height and coplanarity on a micro-BGA.

References

1. H. M. Clearfield, J. L. Young, S. D. Wijeyesekera, and E. A. Logan, "Wafer-lever chip scale packaging: benefits for integrated passive devices," *IEEE Trans. Adv. Packag.* **23**, 247–251 (2000).
2. D. Miller, "Inspection criteria for ball grid arrays," *EE-Eval. Eng.* **38**, 137–145 (1999).
3. S. H. Wang, C. J. Jin, C. J. Tay, C. Quan, and H. M. Shang, "Design of an optical probe for testing surface roughness and micro-displacement," *Precis. Eng.* **25**, 258–265 (2001).
4. S. H. Wang, C. G. Quan, C. J. Tay, and H. M. Shang, "Surface roughness measurement in the submicrometer range using laser scattering," *Opt. Eng.* **39**, 1597–1601 (2000).
5. D. C. He and L. Wang, "Edge-detection in numerical image-processing," *Int. J. Remote Sens.* **12**, 651–657 (1991).
6. International Organization for Standardization, *Guide to the Expression of Uncertainty in Measurement*, ISO, Geneva (1995).